Advances in Aircraft and Spacecraft Science, *Vol. 7, No. 2 (2020) 91–113*
DOI: https://doi.org/10.12989/aas.2020.7.2.091

Multibody simulation and descent control of a space lander

A. Pagani*[1], R. Azzara[1a], R. Augello[1b] and E. Carrera[1c]

[1]*MuI*[2] *group, Department of Mechanical and Aerospace Engineering, Politecnico di Torino, Corso Duca degli Abruzzi 24, 10129 Torino, Italy*

(Received February 12th, 2019, Revised June 14th, 2019, Accepted September 15th, 2019)

Abstract. This paper analyzes the terminal descent phase of a space lander on a surface of a celestial body. A multibody approach is adopted to build the physical model of the lander and the surface. In this work, a legged landing gear system is considered. Opportune modelling of the landing gear crashbox is implemented in order to accurately predict the kinetic energy. To ensure the stability of the lander while impacting the ground and to reduce the contact forces that arise in this maneuver, the multibody model makes use of a co-simulation with a dedicated control system. Two types of control systems are considered; one with only position variables and the other with position and velocity variables. The results demonstrate the good reliability of modern multibody technology to incorporate control algorithms to carry out stability analysis of ground impact of space landers. Moreover, from a comparison between the two control systems adopted, it is shown how the velocity control leads to lower contact forces and fuel consumption.

Keywords: multibody simulation; space landers; landing stability; control system.

1. Introduction

As reviewed by Badescu (2009), the space is very rich in material and energy resources, which are different from those common on the Earth surface. The space mining industry could generate a new economic boom thanks to the extraction of materials that are rare on Earth. The description of this is documented by Sullivan and McKay (1991). As reported by Larson and Pranke (1999), in a space mission many difficulties arise due mainly for the low gravity, for the radiation and for the little knowledge about the scenario in which machines will operate. Furthermore, in the last decade, the interest in the space colonization has become increasingly strong not only for the exploitation of resources, but also for establishing permanent bases. Exploration of solar system bodies has been attracting the attention of the

*Corresponding author, Associate Professor, E-mail: alfonso.pagani@polito.it
[a]Ph.D. student, E-mail: rodolfo.azzara@polito.it
[b]Ph.D. student, E-mail: riccardo.augello@polito.it
[c]Professor, E-mail: erasmo.carrera@polito.it

http://www.techno-press.org/?journal=aas&subpage=7 ISSN: 2287-528X(Print), 2287-5271(Online)

scientific community, see for example (O^ Neill 1974). Many countries and organizations are carrying out extensive space researches. For the realistic realization of these objectives, an accurate design of the exploration spacecraft is needed. As a matter of fact, mathematical models are needed to ensure the success of the robotic space mission, as described by Dong *et al.* (2005).

The part of the spacecraft, whose task is the descent and landing on the surface of a celestial body, is the lander. Griffin (2004) provided an excellent and exhaustive work on the design process of this kind of vehicles. The history of space explorations involving robotic missions with landers is fairly recent, as mentioned by Siddiqi (2010). The last 40 years have seen the successful implementation of various missions, among which are cited: Viking 1 (which result are provided by Mutch *et al.* (1976)), Mars Pathfinder (described by Golombek *et al.* (1997)), Phoenix Mars (data analyses reported by Kounaves *et al.* (2010)), Venera (which results are described by Surkov *et al.* (1983)), Spirit (an overview is reported by Arvidson *et al.* (2006)), Opportunity (an overview is described by Squyres *et al.* (2006)), Rosetta (described by Glassmeier *et al.* (2007)). To guarantee the success of the mission, the lander must be able to land on the ground softly and in a stable way, avoiding both high impact forces that could fail the structure and lead to a possible vehicle overturning. A landing phase in the most stable condition possible is well described by Chu (2006). As mentioned by De Lafontaine (1992), researchers have been dedicated to the development of mathematical models to realize the simulation of a soft landing. Ramanan and Lal (2005) proposed an idea of analysis of optimal strategies for soft-landing on the Moon. The realization of a soft landing, described by Martella *et al.* (2008), is a challenging task both because the landing operation is done in an unknown site and because the vehicle could be randomly oriented as regards the flight path. These issues, have been analyzed by Stio *et al.* (2017) and the problem was overcome by performing a DOE (Design of Experiments) analysis to evaluate the worst possible scenario and ensuring the lander stability in that particular condition. Furthermore, the behavior of the lander in the presence of a local obstacle was also shown.

Because the system is characterized by large displacements, the equations of governance are no longer linearizable, and therefore the multibody methodology, as reported by Gontier and Li (1995), turns out to be a good solution both in terms of mathematical complexity and accuracy to study these systems. Multibody codes are widely used in several engineering fields. Banerjee (2003) described the analyses on space flight using multibody dynamics, Sherman *et al.* (2011) developed open source code, Simbody, for the multibody analysis in the biomedical fields, modeling prosthetic, biomolecular and neuromuscular systems. Besides, Dallali *et al.* (2013) analyzed the movements of a humanoid robot, proving the multibody approach efficiency in the robotic engineerin. Blundell and Harty (2004) used multibody approach to define suspension systems behavior. The multibody method, described by Von Schwerin (2012), allows observing how the system behaves during the maneuvers and modifying both the structural configuration of the lander and some parameters involved in a very simple way. As described by Schiehlen *et al.* (1990), given the system complexity to be studied, it is very useful and practical to use a multibody approach. In the literature, much attention has been focused on the development of efficient control systems in order to guarantee an increasingly reliable descent phase. Control system configuration and control logic are verified

by using computer simulations. For example, AlandiHallaj and Assadian (2017) proposed a Multiple-Model Predictive Control to be used for soft-landing on an irregular shape asteroid. Rew *et al.* (2014) described a control system design to be implemented in their Korean lunar lander demonstrator.
The software used for this work is ADAMS (Adams 2003), which, thanks to its multidisciplinary nature, allows to realize co-simulations with the Matlab/Simulink (Simulink and Natick 1993) to introduce the control in the various simulations. The control system is introduced with the purpose of guaranteeing the lander to land safely and successfully on the surface. All the lander components are built within the ADAMS code, considering for this preliminary study all the rigid elements without introducing flexibility. The present paper wants to investigate the lander downhill phase, and in particular the control systems design to appropriately perform the maneuvers. The goal is to ensure a landing in the most stable condition possible, but also to guarantee acceptable impact strength values from a structural point of view. The control system is able to rule the activation time of the thrusters, opportunely applied to the lander model, being able to stabilize it before ground impact. In this work, thrusters are simulated by translational forces directed towards the surface, so that there are no risks to contaminate the ground when the debris is ejected. The description of thrusters used for aerospace applications is reported by Hofer *et al.* (2006) and by Desai *et al.* (2011).
In the design of a lander, particular attention should be paid to the landing gear, which represents a critical and crucial system. Nowadays, there are four types of landing gear systems for space landers, including airbags structure landing gear (Cadogan *et al.* 2002), legged landing gear system, skycrane and wheel landing system (Kornfeld *et al.* 2014), and crushable structure landing system (Bayle *et al.* 2011). In this work, the legged landing gear system was chosen. As an example, Zheng *et al.* (2018) used this class of landing gear in their dynamic analyses of a lunar lander during soft-landing. The legged landing gear system has some advantages: 1) easy control of the attitude and position of lander during landing; 2) minimum overload during landing; 3) more effectively protect the precision instrument and 4) more successful case in comparison with the other landing systems.
The results will show how stability is guaranteed during the descent phase and how a control with position and velocity variables allows reducing both the value of the contact forces and the fuel consumption. This article is organized as follows: (i) first a brief review of a multibody dynamics formulation is reported in Section 2; (ii) then, some description and introductory information are given in Section 3, including a brief outline of the lander model; (iii) next, stability analysis and control systems are introduced in Section 4; (iv) hence, the results discussed in Section 5 to prove the efficacy of the multibody approach; (iv) finally, in Section 6 the main conclusions are drawn.

2. Multibody dynamics

The use of computational tools to simulate mechanical systems is very advantageous in the field of computer-assisted engineering. The development of such software has allowed performing more detailed analyses on the complex dynamics of the systems. These simulation

codes are based mainly on the principles of Lagrangian dynamics. Although the theory of principles was already known in the eighteenth century, until recently, the complexity of the Lagrangian equations did not allow the study of various applications. With the development of high-speed computers and new sophisticated methods of numerical calculation for the resolution of algebraic and differential equations, the actual use of multibody programs was possible.
As reported by Pagani *et al.* (2019), the multibody analysis is based on the Euler-Lagrange equation:

$$\frac{d}{dt}\left(\frac{\partial \mathbf{L}}{\partial \dot{\mathbf{u}}}\right) - \frac{\partial \mathbf{L}}{\partial \mathbf{u}} + \sum_{k=1}^{m} \frac{\partial \mathbf{\Phi}_k}{\partial \mathbf{u}} \boldsymbol{\lambda}_k = \mathbf{Q} \tag{1}$$

where $\mathbf{L}$ is the Lagrangian of the system, given by the difference between the kinetic and potential energies of the rigid body, $\mathbf{u}$ is the vector of generalized displacements, while $\boldsymbol{\lambda}$ are the Lagrange multipliers, m is the number of constraint equations, $\mathbf{\Phi}$ represent the constraints equations and $\mathbf{Q}$ is the vector of the generalized external forces.
In the case of rigid bodies, ADAMS implements these parameters in every system component, building a set of equations in the following shape:

$$\mathbf{M}\ddot{\mathbf{u}} + \dot{\mathbf{M}}\dot{\mathbf{u}} - \frac{1}{2}\left(\frac{\partial \mathbf{M}}{\partial \mathbf{u}}\dot{\mathbf{u}}\right)^T + \mathbf{f_g} + \mathbf{\Phi}\boldsymbol{\lambda} = \mathbf{Q} \tag{2}$$

where $\mathbf{M}$ is the mass matrix and $\mathbf{f_g}$ is the generalized gravitational load vector.
Once the constraint equations in $\mathbf{\Phi}$ are replaced, a resolvable second order system containing Lagrange multipliers is obtained. ADAMS uses ADAMS-Bashforth and ADAMS-Moulton methods to integrate a set of ordinary differential equations. This method leads to the integration of only a selected portion of the degrees of freedom, which change most during the simulation, adopting the Newton-Raphson method. For further information, see (Arbor *et al.* 2004).

3. Multibody model of the lander

This section describes the multibody model of the space lander prior to integration with the control system. This model is depicted in Fig. 1 for the sake of clarity. Note that the entire structure is made of aluminium for simplicity. Although this choice does not affect the validity of the analysis.
The lander is composed of a chassis, two panels representing the solar arrays, four legs and four foot-pads. Figure 2 details all the important components of the multibody model. In Fig. 2(a), the ADAMS model of the lander is shown, while in Fig. 2(b) the introduced joints are reported. Table 1 shows the characteristics of every body part. The joints connecting the different parts are depicted in Fig. 2(b) and described in Table 2. Each leg is subdivided into an upper and a lower tube that slides into each other. In order to absorbe the kinetic energy at the impact on the ground and avoid re-bounce, a collapsible element, defined as crashbox, is introduced within the upper and lower cylinders. For each leg, the crashbox is simulated in ADAMS via a resistance that acts between the two cylinders. The equation that simulates the crashbox behavior in ADAMS is divided in two parts. The first part takes action when no

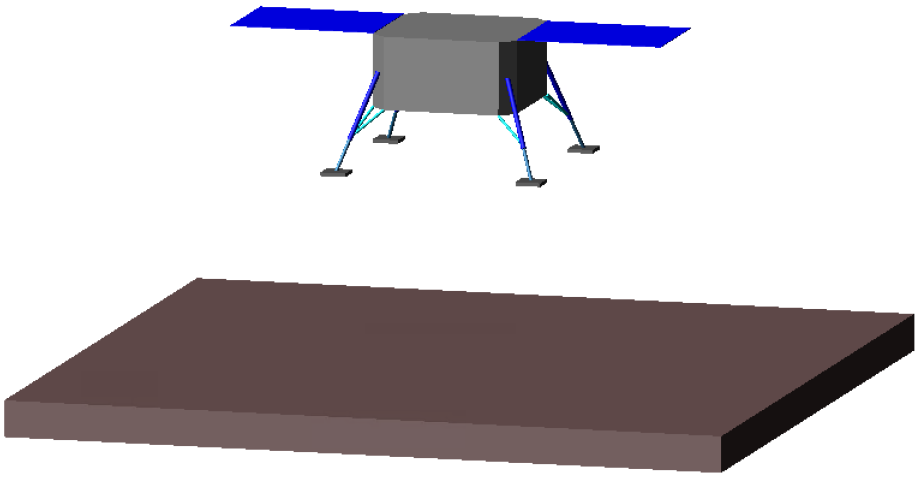

Fig. 1 Lander and road geometry in multibody model.

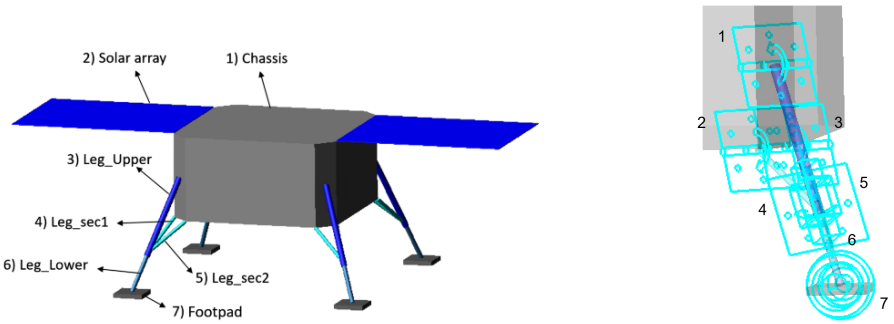

(a) ADAMS model (b) Joints

Fig. 2 Multibody model of the lander.

Table 1 Multibody Parts. CM position is in [mm], referring to the origin of the working grid.

Multibody components				
Part	CM X position	CM Y position	CM Z posiiton	Weight [kg]
Chassis	0.000	0.000	101.5	900.0
Leg Upper	211.5	−211.5	10.50	0.085
Leg Lower	254.2	−254.2	−110.3	0.024
Leg sec1	200.0	−220.0	−35.00	0.016
Leg sec2	220.0	−200.0	−35.00	0.016
Footpad	271.5	−271.5	−164.5	0.150

Table 2 Joint connectors.

Joint connectors			
Joint	Type	First body	Second body
1	Revolute	Leg Upper	Chassis
2	Revolute	Leg sec1	Chassis
3	Revolute	Leg sec2	Chassis
4	Revolute	Leg sec1	Leg Upper
5	Revolute	Leg sec2	Leg Upper
6	Translational	Leg Lower	Leg Upper
7	Spherical	Leg Lower	Footpad
8	Fixed	Road	Ground

contact occurs, and it defines the behavior of the crashbox as a spring. The second part takes action when there is the lander-ground contact and simulates the real crashbox behavior, using parameters that comes out from experimental tests. The theoretical functioning of a crashbox is widely described in the paper of Stio *et al.* (2017).
The introduction of the control system is implemented in ADAMS through the creation of forces, simulating thrusters. They are activated with the purpose of straightening the lander and make it land in the most stable condition possible. The positions of these forces are reported in Fig. 3 in the two cases. These forces will be taken as input from the control

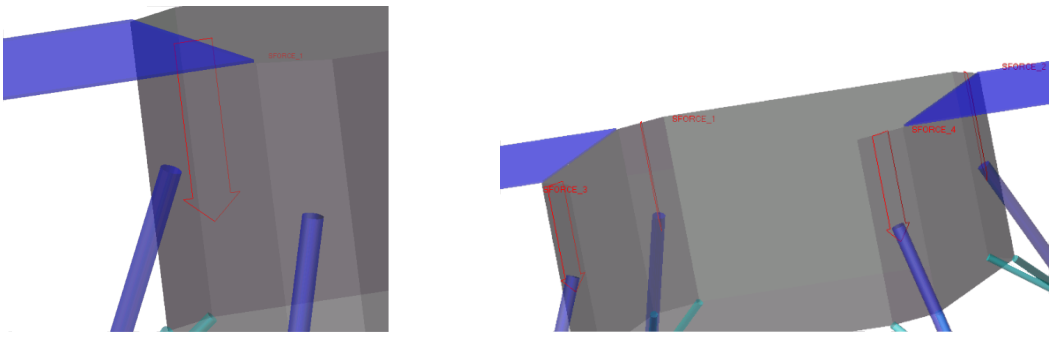

(a) 2D control by two thrusters (b) 3D control by three thrusters

Fig. 3 Forces representing thrusters.

system and a force will be activated or not according to the relative configuration between the lander and the ground.

4. Control system

The main focuses of this work are the descent phase simulation to the ground and the control to be implemented in order to allow the more stable and soft landing. Different configurations are simulated with different control systems. Several scenarios were analyzed to validate and verify both the reaction time and the realiability of the control system. These

control systems have been created using thrusters that make the lander impact on the ground in the best condition (neither overturning or need for heavy and expensive crashbox). The three different control systems implemented are reported hereinafter. The Matlab/Simulink software is used to implement the control systems. Thanks to the multidisciplinarity of the ADAMS software, it is possible to implement the Simulink control system and start a co-simulation between the two software tools. The idea behind the construction of the block diagram is to make a control system as simple as possible, but effective for the cases under consideration. The control system requires the relative position between the lander and the ground, see Fig. 4. As an output, it will return the value of the trusters' forces. 100 N if the thruster has to be activated to stabilize the lander, otherwise 0 N.
Figure 5 shows the block diagram related to position (P) control system on the Y-Z plane.
The block diagram representing the position control system on X-Y-Z in the 3D space is

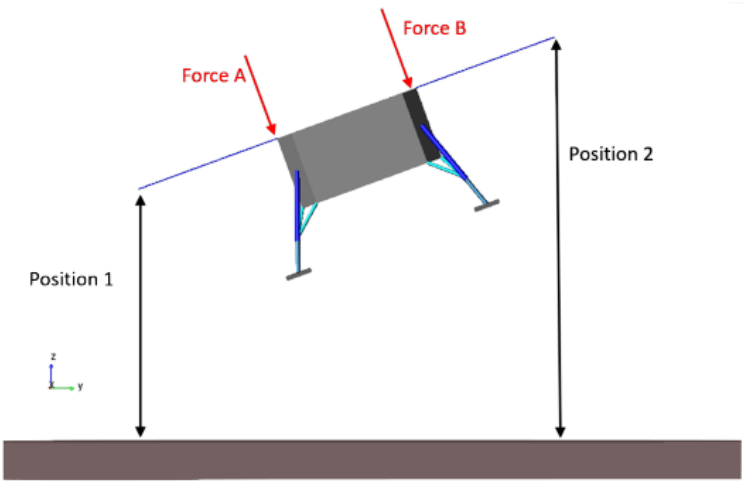

Fig. 4 Initial configuration of the lander.

very similar to that of Fig. 5 with the only difference that now the specific input information are 4, as well as the output forces values of the control system. In Fig. 6, the Proportional-Derivative (PD) type control system on Y-Z is shown. A velocity control was also added to improve the lander stabilization during the descent phase and to reduce contact forces on impact with the ground. Furthermore, this allows reducing consumption and to avoid the lander oscillations and other problems related to this. The derivative action (D) was added with the idea of rapidly compensating the error signal variation between the two positions. Inside the function block (fnc) of Matlab/Simulink in Fig. 6, the script that defines the activation of one force rather than another is defined and it is not reported here for brevity sake. In contrast, for completeness reason, Fig. 7 shows the ADAMS logic to implement co-simulation with the control system.

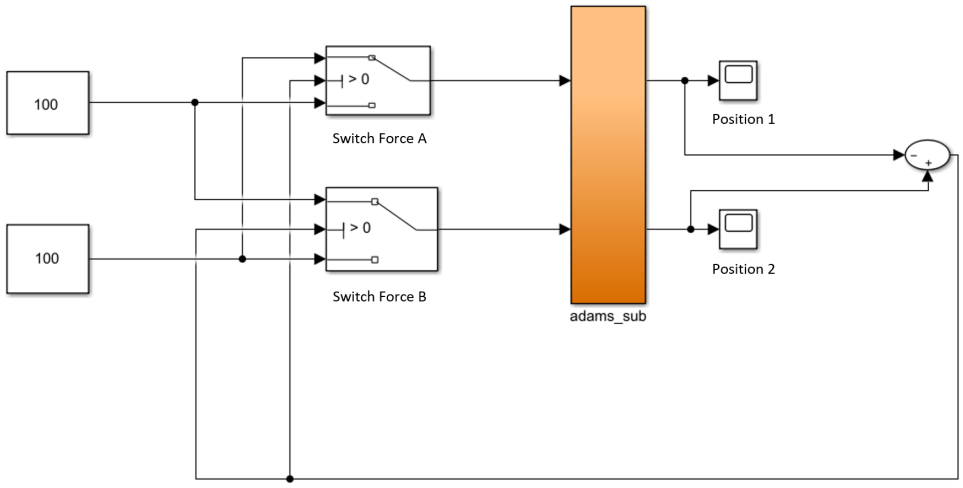

Fig. 5 Position control system on the Y-Z plane.

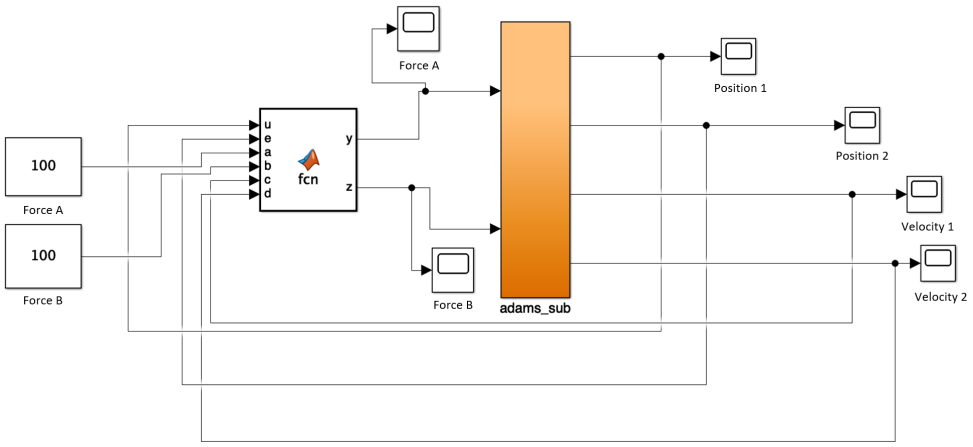

Fig. 6 PD type control system on Y-Z.

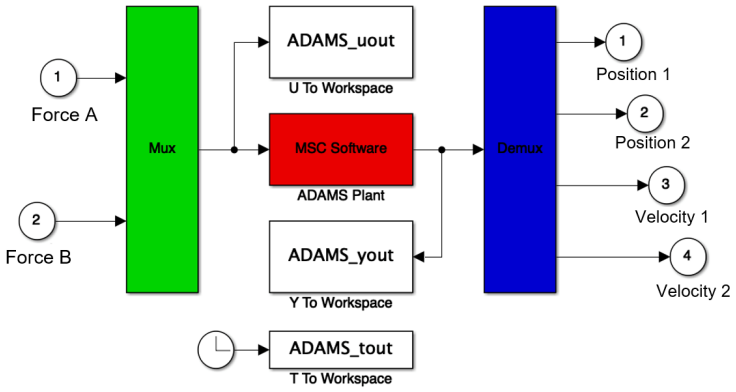

Fig. 7 ADAMS logic of co-simulation.

5. Numerical results

Different analysis configurations are considered for validating the proposed model and for assessing robustness of the control systems. Each configuration differs in the lander relative position with respect to the ground and in the control system architecture. In the first case, a P control is used, whereas in the second case a PD control is employed to increase the efficiency and the complexity. Also, a proper comparison of P and PD systems is carried out.
Different activation instants are considered depending on the distance between the lander and the ground, ranging from 0.8 m to 2.8 m. In all the cases, the lander has an initial velocity along -Z equal to 1 m/s and an initial angular velocity around + Y of 5 degrees/s.

5.1 2D landing with P control system

The first configuration has the following characteristics:

1. Lander inclined by 20° around the -X, see Fig. 4;
2. Position control system on the Y-Z plane.

Figure 8 shows the impact of the lander in the case in which the control system is not active. In the case, without control, the lander in an unstable condition, risking to overturn. In addition to the stability condition, landing without control results to be disadvantageous because of the impact forces and of the fuel consumption. In the case without control, in fact, the forces are always activated, while in the case with the control, they are activated only when necessary.
Figure 9 shows the landing phase when P control system is active. In particular, both impact and final configurations are depicted in the figure. Furthermore, Fig. 10 shows the thrust forces over the time and for the entire duration of the landing. Finally, for completeness reasons, Fig. 11 gives the positions 1 and 2 as a funcion of time, from 0 to 0.4 s.

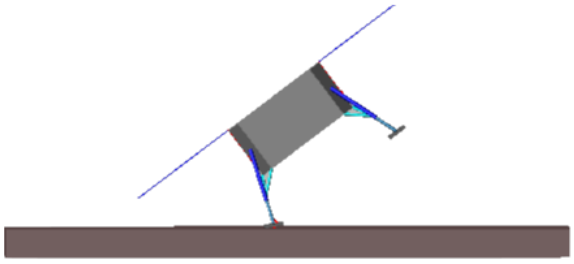

Fig. 8 2D ground impact of the lander with no control.

(a) Ground impact (b) Final condition

Fig. 9 2D landing of the lander with P control system.

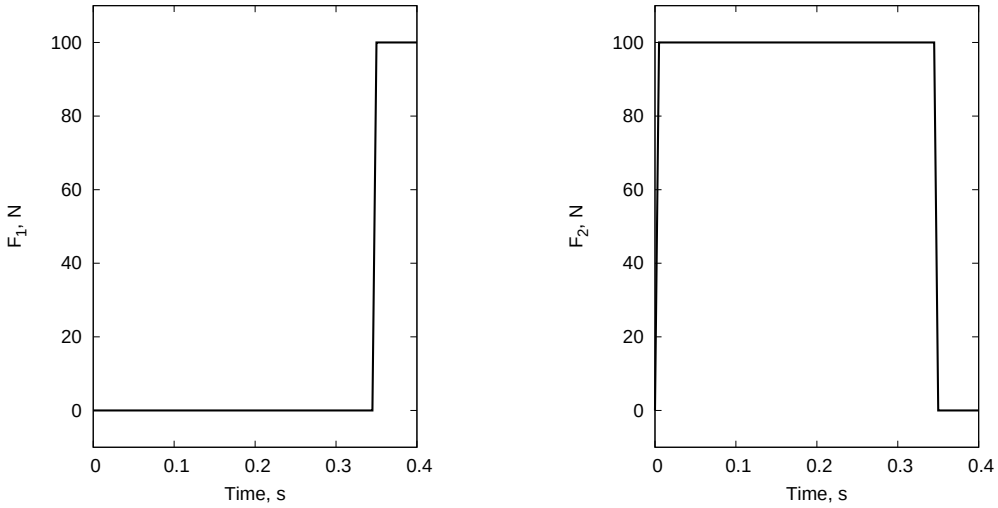

Fig. 10 Thruster forces of the 2D landing with P control system.

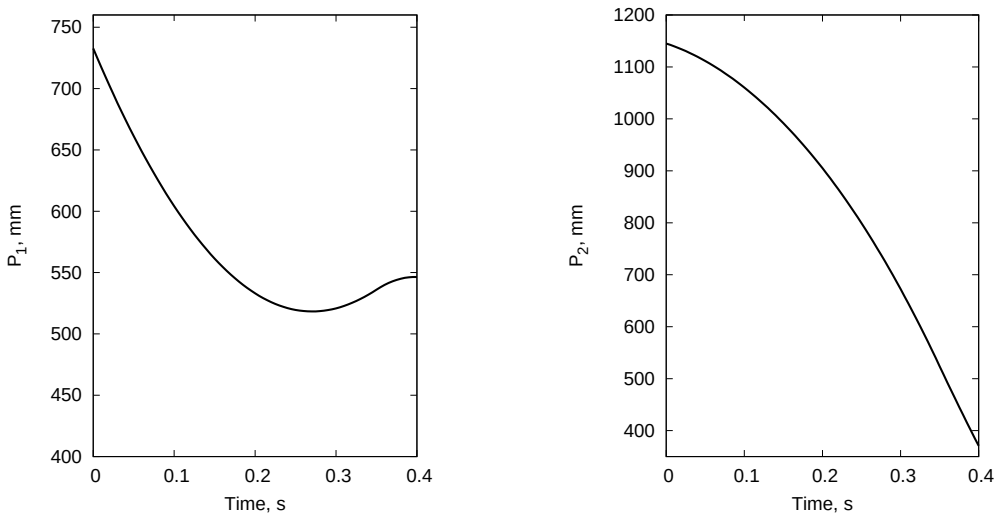

Fig. 11 Positions 1 and 2 during the landing phase in the case of 2D land and P control system.

5.2 3D landing with P control system

The second configuration has the following characteristics:

1. Lander inclined by 20° around -X and 20° around Z, see Fig. 12;
2. Road inclined by −10° around X, see Fig. 12;
3. Position control system on X-Y-Z.

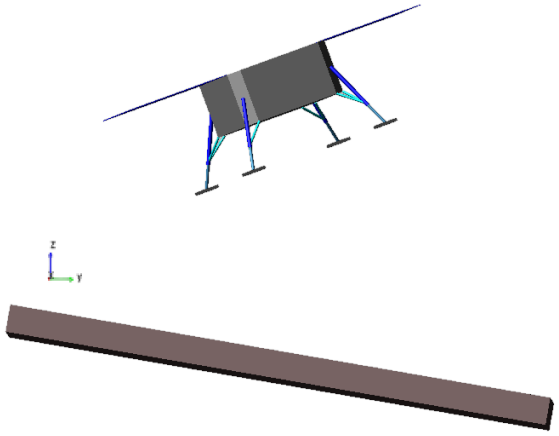

Fig. 12 Initial configuration of the lander in the case of 3D land and P control system.

Figure 13 shows the impact of the lander in the case in which the control system is not active. The case without control leads to an unstable condition with an inevitable overturning of

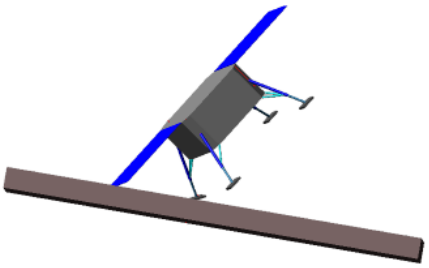

Fig. 13 3D ground impact of the lander with no control.

the lander. Figure 14 shows the landing phase when a 3D P control system is active. In this

(a) Ground impact (b) Final condition

Fig. 14 3D landing of the lander with P control system.

case it is observed a greater stabilization on landing compared to the previous case. The advantage in consumption terms is even more evident, as the thrusters' forces are now 4. In the case without control, the thruster forces are always equal to the maximum value. In the case with control, the thrusters forces are reported during the simulation in Fig. 15. The graphs of the positions as a function of time in Fig. 16 are shown.

5.3 Comparison between P and PD control systems

This section discusses a comparison between the use of P and PD controls in the case of activating the control system at a higher altitude. This configuration has the following characteristics:

1. Lander inclined by 20° around -X, see Fig. 17;
2. Fall height of 2.8 m and initial velocities equal to previous cases.

The impact configurations in the case without control is reported in Fig. 18. Figure 19 shows 2D landing of the lander with both P and PD control system. It is immediately

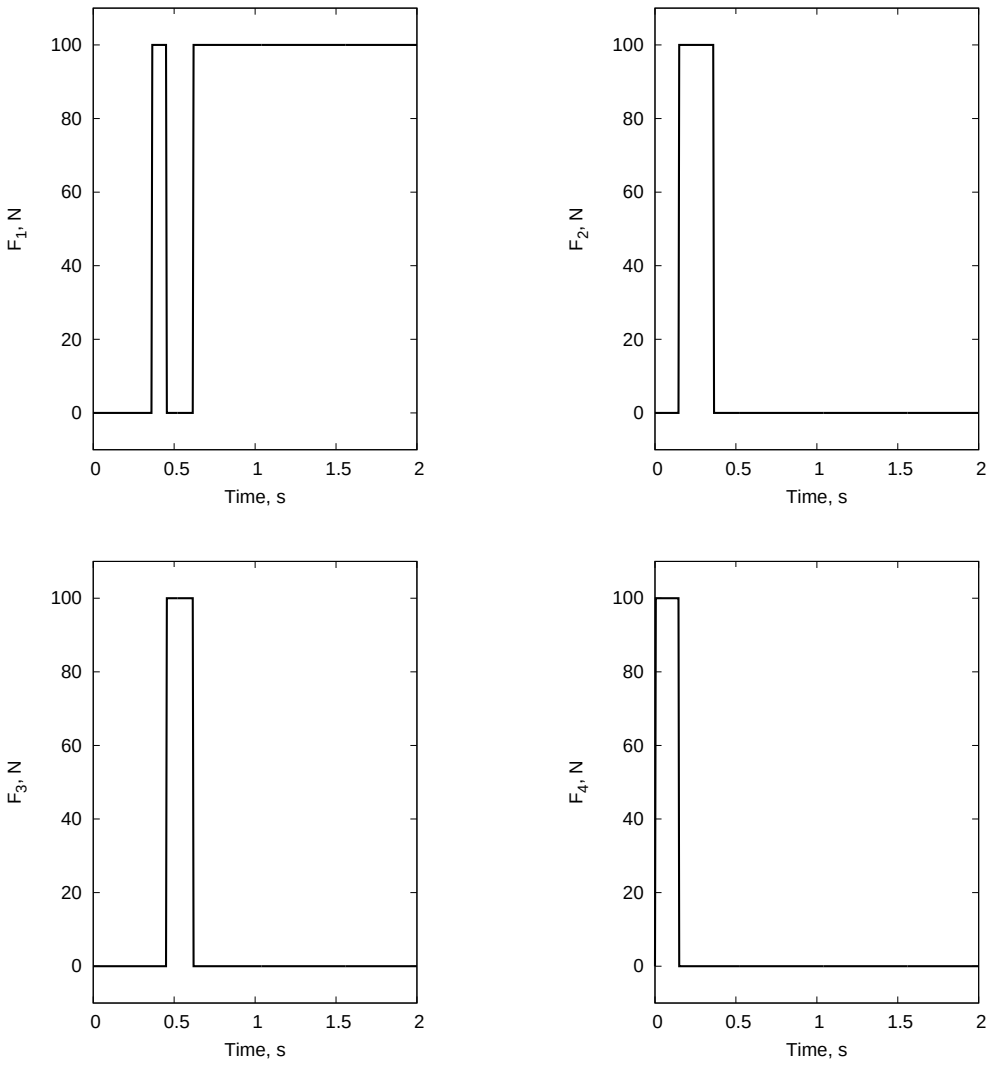

Fig. 15 Thruster forces of the 3D landing with P control system.

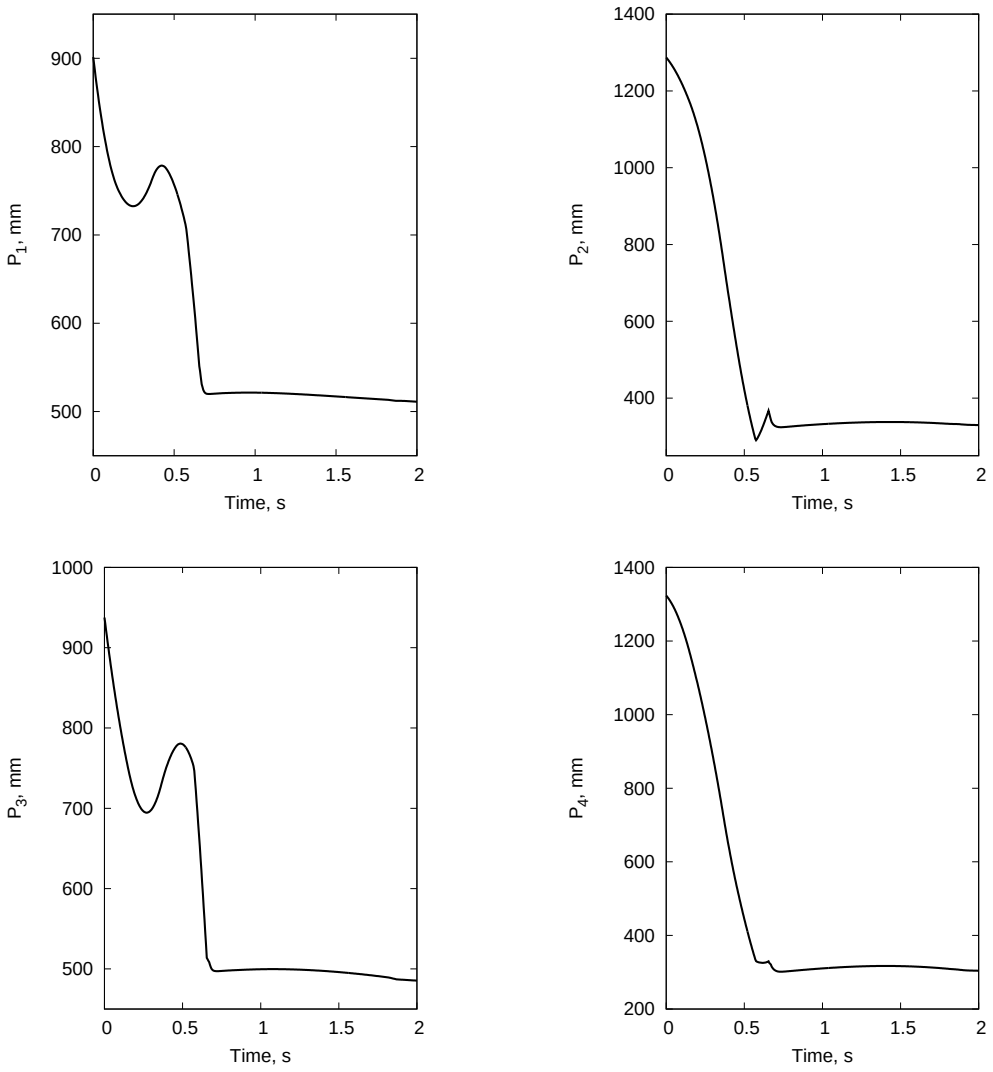

Fig. 16 Positions during the landing phase in the case of 3D land and P control system.

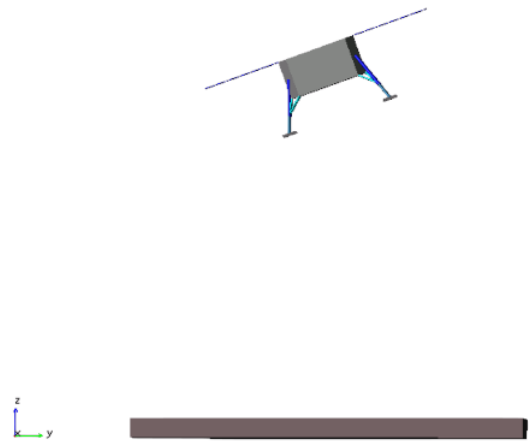

Fig. 17 Initial configuration of the lander in the comparison case between P and PD control system.

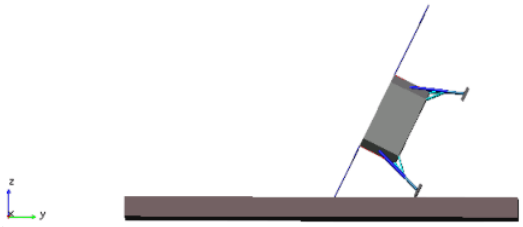

Fig. 18 Ground impact of the lander in the comparison case between P and PD control system with no control.

(a) Ground impact with P control system

(b) Ground impact with PD control system

Fig. 19 Comparison between P and PD control systems.

Table 3 Contact forces in the case with P control and without control.

–	*P control*	*No control*
Contact Force max [N]	19425	30120

Table 4 Benefits introduced with the PD control system.

–	*P control*	*PD type control*
Force 1 activation time [s]	0.53	0.23
Force 2 activation time [s]	0.45	0.25
Total time activation time [s]	0.98	0.45
Contact Force max [N]	19425	5408

highlighted that the PD control system leads to better stabilization. The different landing phases in the case of P control are shown in Fig. 20 along with the thrusters' forces. In addition to the consumption advantage, in the Table 3 the decrease in contact forces is shown compared to the case without control. It is evident that the contact forces on impact with the ground in the case without control are higher than the ones from the case with position control. This is already a considerable advantage, but these values are still very high so that heavy, expensive and complicated crashboxes need to be designed. For this reason and also to reduce the effects related to the lander oscillations due to the activation of thrusters, a PD control needs to be taken into account as discussed in the following.
Figure 21, instead, shows the landing phases in the case of PD control. For completeness reasons, the graphs of the positions 1 and 2 are shown as a function of time in Fig. 22 in the case of P system. The graphs of the thrusters' forces in the case with control are shown in Fig. 23, highlighting a more significant advantage related to the reduction in consumption compared to the case without control. Moreover, there is also a considerable contact force values decrease compared to the case with only position control. This allows to design a simpler crashbox and to reduce the forces acting on the lander structure. Finally, Fig. 24 and 25 show the trends of the positions and velocities for this case.
A more linear trend of the lander during the downhill phase compared to the case without velocity control can be observed. This allows minimizing the oscillations caused by the thrusters activation and leads to better stabilization of the lander. From this last scenario presented, the usefulness and the need to introduce a control also on the velocity is shown both to have advantages on consumption and to decrease the contact forces, which are too high in the case with only position control. Finally, the benefits introduced with the PD control system are shown in Table 4.

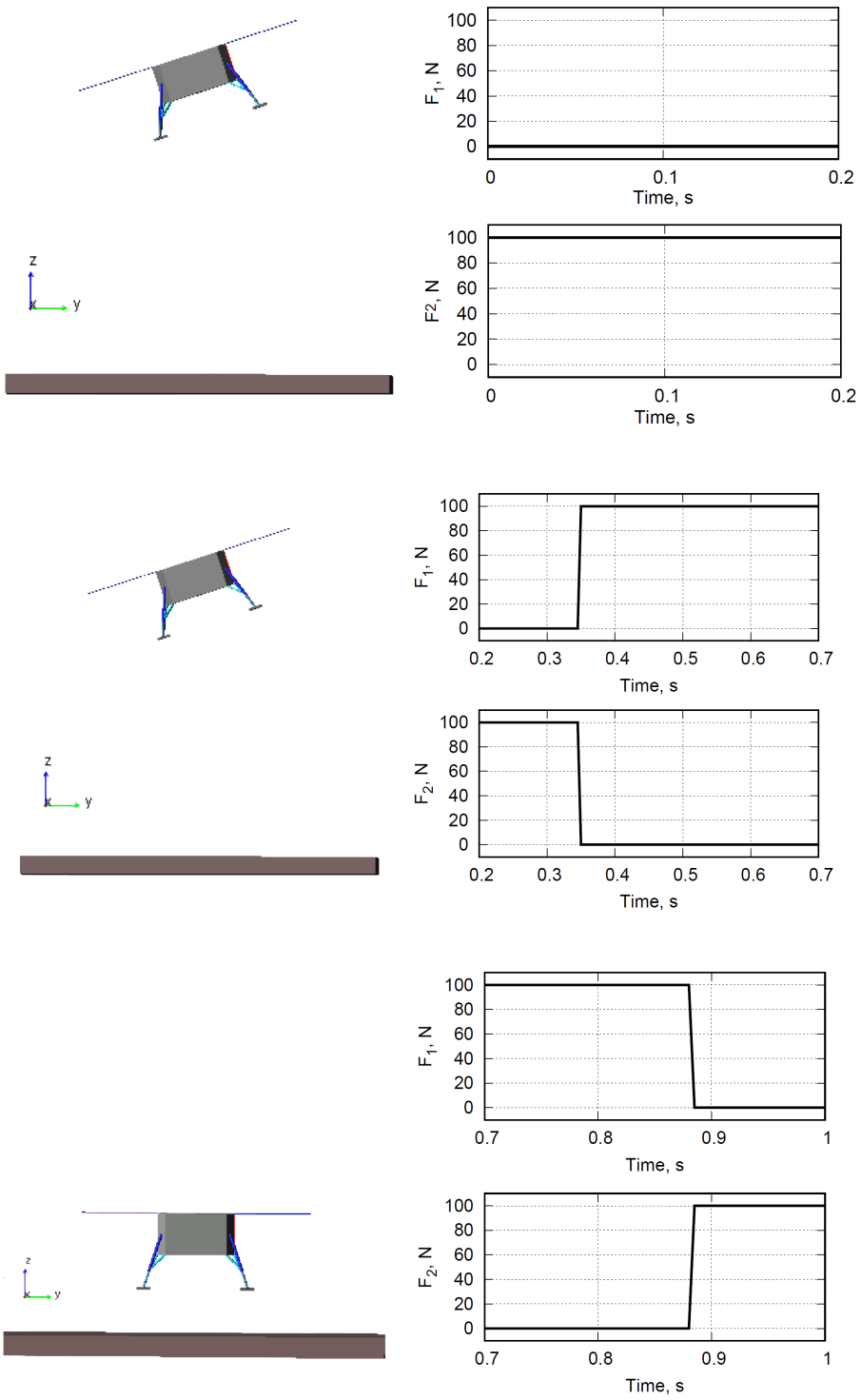

Fig. 20 Landing phase sequence in the comparison case between P and PD with P control system.

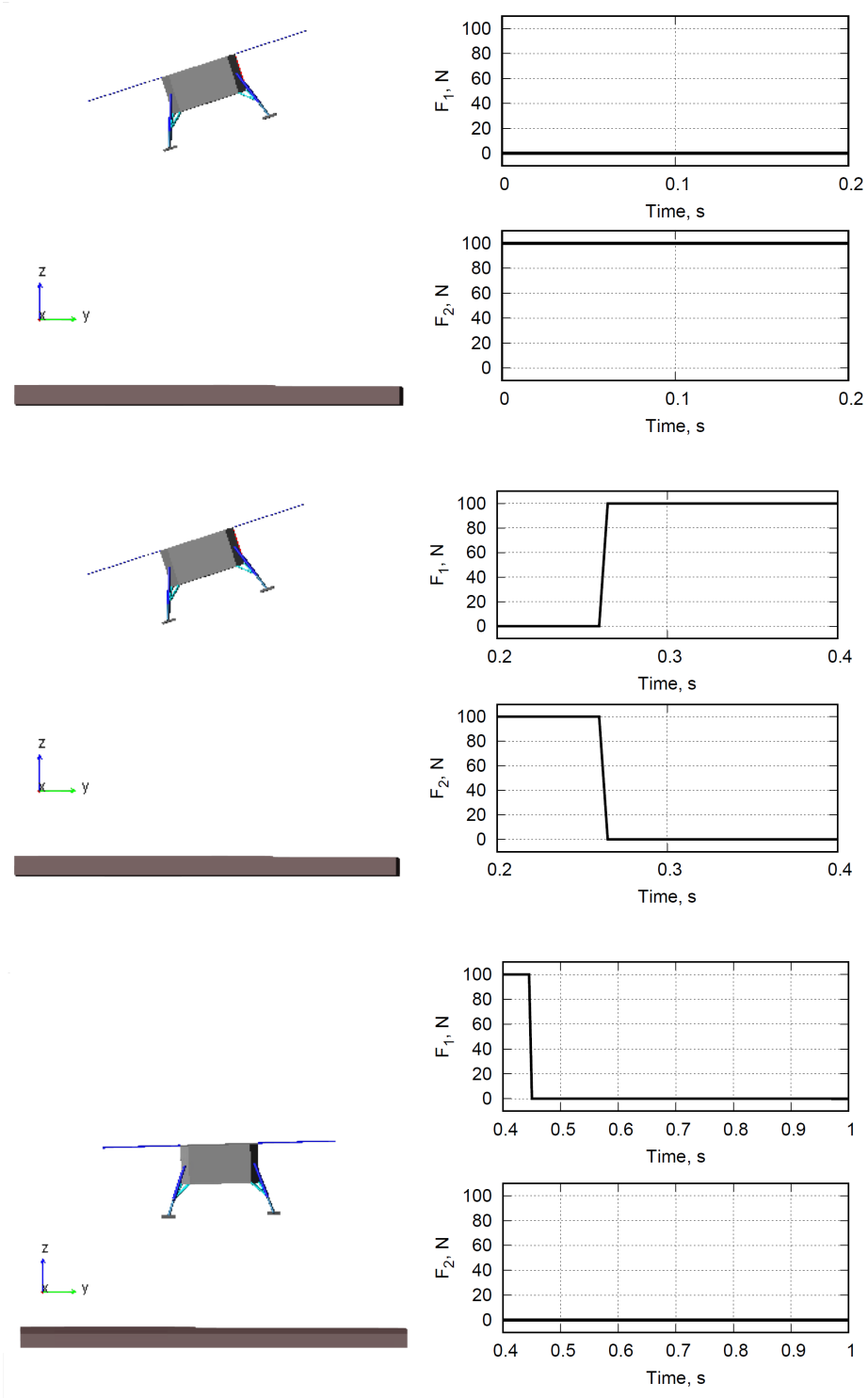

Fig. 21 Landing phase sequence in the comparison case between P and PD with PD control system.

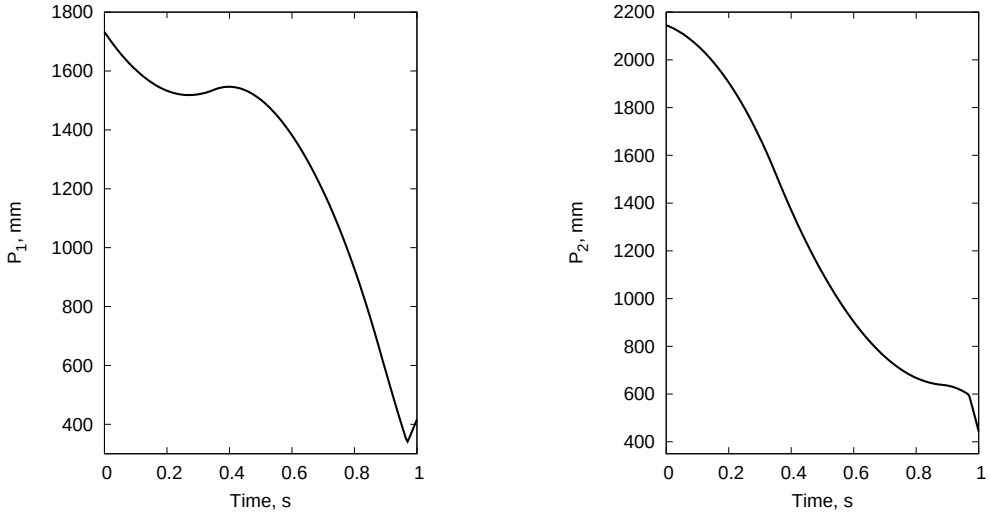

Fig. 22 Positions 1 and 2 during the landing phase in the comparison case between P e PD with P control system.

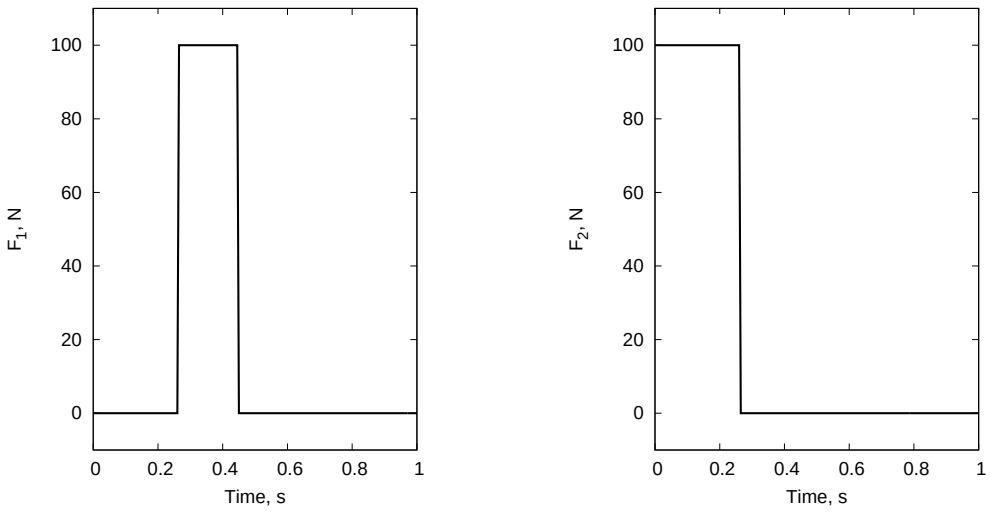

Fig. 23 Thruster forces of the comparison case between P and PD control with P control system.

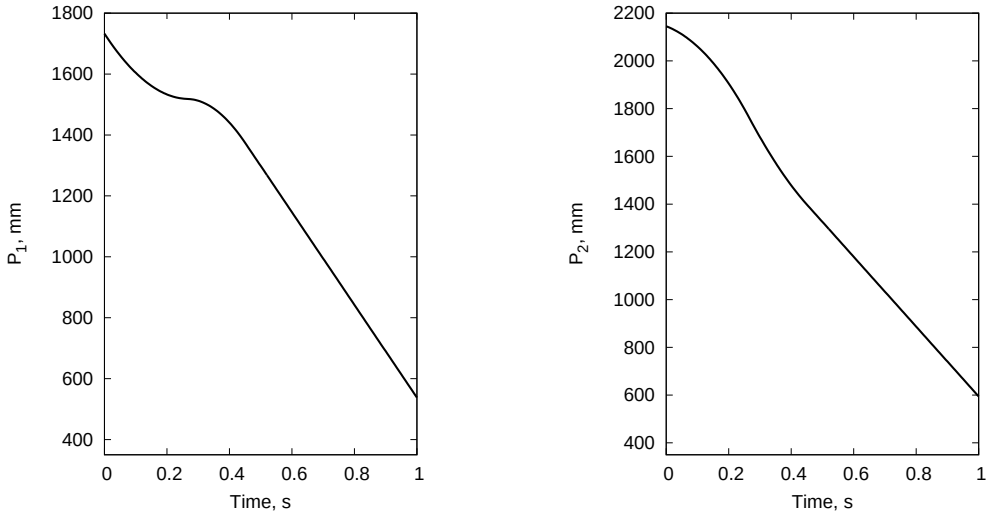

Fig. 24 Positions 1 and 2 during the landing phase in the comparison case between P and PD control with PD control system.

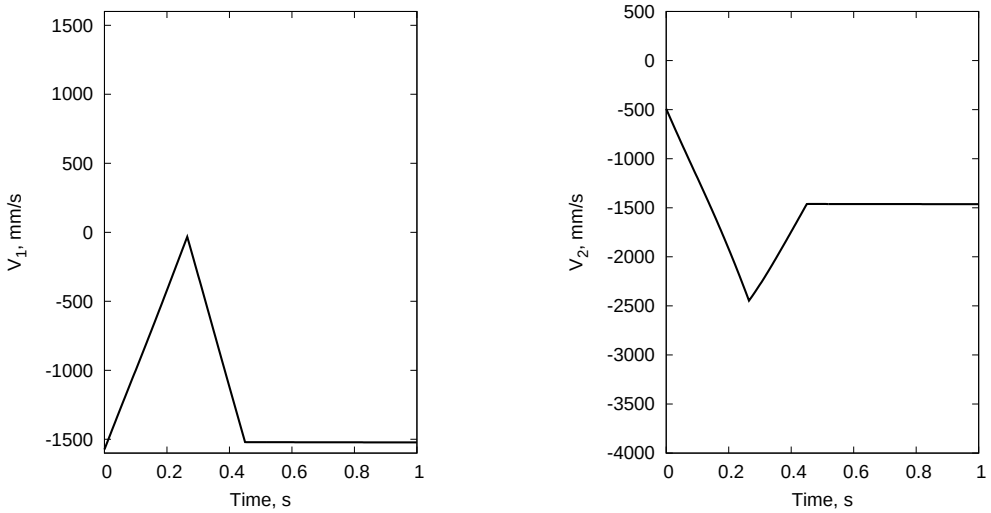

Fig. 25 Positions 3 and 4 during the landing phase in the comparison case between P and PD control with PD control system.

6. Conclusions

In this work, a multibody approach to study the lander stability during the landing phase on a spatial body is proposed. In particular, the control system design along with its characteristics is analyzed. The descent phase study turns out to be very important because it is fundamental for the success of the mission and for its criticalities, which is the reason we need to increase its reliability. The risks that can be recovered in this phase are many, for example, the low gravity of the celestial body, the nature of the land that can be only supposed and natural phenomena that can disturb the lander. Once the lander model was built and the control system was implemented, several simulations were performed with different scenarios, evaluating the stabilization, consumption and impact forces. These forces are important both for the crashbox design and for assessing the structural strength of the entire lander. Through the simulations, the effectiveness of the co-simulation between the ADAMS code and the Matlab/Simulink software was demonstrated. The control was carried out through thrusters directed towards the planet surface where want to land both overcome the low gravity issue and not to contaminate the ground. The use of a PD control was found to be advantageous compared to the one with only position variable.

References

Adams, M. (2003), "MSC. Software Corporation", *Ann Arbor, Michigan*.

AlandiHallaj, M. and Assadian, N. (2017), "Soft landing on an irregular shape asteroid using Multiple-Horizon Multiple-Model Predictive Control", *Acta Astronautica*, **140**, 225–234.

Arbor, A., Negrut, D. and Dyer, A. (2004), "Adams/solver primer", .

Arvidson, R., Squyres, S., Anderson, R., Bell, J., Blaney, D., Brueckner, J., Cabrol, N., Calvin, W., Carr, M., Christensen, P. *et al.* (2006), "Overview of the spirit Mars exploration rover mission to Gusev Crater: Landing site to Backstay Rock in the Columbia Hills", *Journal of Geophysical Research: Planets*, **111**(E2).

Badescu, V. (2009), *Mars: prospective energy and material resources*, Springer Science & Business Media.

Banerjee, A. (2003), "Contributions of multibody dynamics to space flight: a brief review", *Journal of Guidance, Control, and Dynamics*, **26**(3), 385–394.

Bayle, O., Lorenzoni, L., Blancquaert, T., Langlois, S., Walloschek, T., Portigliotti, S. and Capuano, M. (2011), "Exomars entry descent and landing demonstrator mission and design overview", *Nasa Solar System*.

Blundell, M. and Harty, D. (2004), *Multibody systems approach to vehicle dynamics*, Elsevier.

Cadogan, D., Sandy, C. and Grahne, M. (2002), "Development and evaluation of the Mars Pathfinder inflatable airbag landing system", *Acta Astronautica*, **50**(10), 633–640.

Chu, C. (2006), "Development of advanced entry, descent, and landing technologies for future Mars missions", in "Aerospace Conference, 2006 IEEE", pages 8–pp.

Dallali, H., Mosadeghzad, M., Medrano-Cerda, G., Docquier, N., Kormushev, P., Tsagarakis, N., Li, Z. and Caldwell, D. (2013), "Development of a dynamic simulator for a compliant humanoid robot based on a symbolic multibody approach", .

De Lafontaine, J. (1992), "Autonomous spacecraft navigation and control for comet landing", *Journal*

of Guidance, Control, and Dynamics, **15**(3), 567–576.

Desai, P., Prince, J., Queen, E., Schoenenberger, M., Cruz, J. and Grover, M. (2011), "Entry, descent, and landing performance of the Mars Phoenix Lander", *Journal of Spacecraft and Rockets*, **48**(5), 798–808.

Dong, S., Luo, Y. and Zhao, Y. (2005), "Practical application and research advances of long-span space structures [J]", *Spatial Structures*, **4**.

Glassmeier, K., Boehnhardt, H., Koschny, D., Kührt, E. and Richter, I. (2007), "The Rosetta mission: flying towards the origin of the solar system", *Space Science Reviews*, **128**(1-4), 1–21.

Golombek, M., Cook, R., Economou, T., Folkner, W., Haldemann, A., Kallemeyn, P., Knudsen, J.M., Manning, R., Moore, H., Parker, T. *et al.* (1997), "Overview of the Mars Pathfinder mission and assessment of landing site predictions", *Science*, **278**(5344), 1743–1748.

Gontier, C. and Li, Y. (1995), "Lagrangian formulation and linearization of multibody system equations", *Computers & structures*, **57**(2), 317–331.

Griffin, M. (2004), *Space vehicle design*, AIAA Education Series.

Hofer, R., Randolph, T., Oh, D., Snyder, J. and De Grys, K. (2006), "Evaluation of a 4.5 kw commercial hall thruster system for NASA science missions", in "42nd AIAA/ASME/SAE/ASEE Joint Propulsion Conference & Exhibit", page 4469.

Kornfeld, R., Prakash, R., Devereaux, A., Greco, M., Harmon, C. and Kipp, D. (2014), "Verification and validation of the Mars Science Laboratory/Curiosity rover entry, descent, and landing system", *Journal of Spacecraft and Rockets*, **51**(4), 1251–1269.

Kounaves, S., Hecht, M., Kapit, J., Gospodinova, K., DeFlores, L., Quinn, R., Boynton, W., Clark, B., Catling, D., Hredzak, P. *et al.* (2010), "Wet Chemistry experiments on the 2007 Phoenix Mars Scout Lander mission: Data analysis and results", *Journal of Geophysical Research: Planets*, **115**(E1).

Larson, J. and Pranke, L. (1999), *Human spaceflight mission analysis and design (Space Technology Series)*, New York: McGraw—Hill.

Martella, P., Buonocore, M., Desiderio, D., Lovera, M. and Portigliotti, S. (2008), "Soft landing on Mars: The GNC tasks in the ExoMars descent module mission", in "7th International ESA Conference on Guidance, Navigation and Control Systems", pages 1–13.

Mutch, T., Binder, A., Huck, F., Levinthal, E., Liebes, S., Morris, E., Patterson, W., Pollack, J., Sagan, C. and Taylor, G. (1976), "The Surface of Mars: There View from the Viking 1 Lander", *Science*, **193**(4255), 791–801.

O^ Neill, G. (1974), "The colonization of space", in "Space Manufacturing Facilities", page 2041.

Pagani, A., Augello, R., Governale, G. and Viglietti, A. (2019), "Drop Test Simulations of Composite Leaf Spring Landing Gears", *Aerotecnica Missili e Spazio*.

Ramanan, R. and Lal, M. (2005), "Analysis of optimal strategies for soft landing on the moon from lunar parking orbits", *Journal of earth system science*, **114**(6), 807–813.

Rew, D., Ju, G., Lee, S., Kim, K., Kang, S. and Lee, S. (2014), "Control system design of the Korean lunar lander demonstrator", *Acta Astronautica*, **94**(1), 328–337.

Schiehlen, W. *et al.* (1990), *Multibody systems handbook*, volume 6, Springer.

Sherman, M.A., Seth, A. and Delp, S. (2011), "Simbody: multibody dynamics for biomedical research", *Procedia Iutam*, **2**, 241–261.

Siddiqi, A.A. (2010), "Competing technologies, national narratives, and universal claims: Toward a global history of space exploration", *Technology and Culture*, **51**(2), 425–443.

Simulink, M. and Natick, M. (1993), "The mathworks", .

Squyres, S., Arvidson, R., Bollen, D., Bell III, J., Brueckner, J., Cabrol, N., Calvin, W., Carr, M., Christensen, P., Clark, B. *et al.* (2006), "Overview of the opportunity mars exploration rover mission to meridiani planum: Eagle crater to purgatory ripple", *Journal of Geophysical Research: Planets*, **111**(E12).

Stio, A., Spinolo, P., Carrera, E. and Augello, R. (2017), "Analysis of landing mission phases for robotic exploration on phobos mars moon", *ADVANCES IN AIRCRAFT AND SPACECRAFT SCIENCE*, **4**(5), 529–541.

Sullivan, T.A. and McKay, D.S. (1991), "Using space resources", *NASA Technical Reports*.

Surkov, Y.A., Moskalyeva, L., Shcheglov, O., Kharyukova, V., Manvelyan, O., Kirichenko, V. and Dudin, A. (1983), "Determination of the elemental composition of rocks on Venus by Venera 13 and Venera 14 (preliminary results)", *Journal of Geophysical Research: Solid Earth*, **88**(S02).

Von Schwerin, R. (2012), *Multibody system simulation: numerical methods, algorithms, and software*, volume 7, Springer Science & Business Media.

Zheng, G., Nie, H., Chen, J., Chen, C. and Lee, H. (2018), "Dynamic analysis of lunar lander during soft landing using explicit finite element method", *Acta Astronautica*, **148**, 69–81.